OIP5-AS1 modulates epigenetic regulator HDAC7 to enhance non-small cell lung cancer metastasis via miR-140-5p

JIAZHUAN MEI, GUIJU LIU, WENHUI WANG, PENG XIAO, DAN YANG, HUA BAI and RUIJUN LI

Department of Oncology, People's Hospital of Zhengzhou, Zhengzhou, Henan 450000, P.R. China

Abstract. Long non-coding RNAs have been reported to be involved in non-small cell lung cancer (NSCLC) progression. However, whether Opa-interacting protein 5 antisense RNA 1 (OIP5-AS1) serves a role in NSCLC remains unclear. Bioinformatics analysis of The Cancer Genome Atlas datasets showed clinical significance and relevance of OIP5-AS1 in NSCLC. Western blotting and reverse transcription-quantitative PCR revealed protein and RNA expression levels of the genes [including *OIP5-AS1*, microRNA (miR)-140-5p, histone deacetylase 7 *(HDAC7)* and vascular endothelial growth factor A *(VEGFA)*]. Direct associations between the genes (miR-140-5p and OIP5-AS1, or miR-140-5p and HDAC7) were confirmed using a dual-luciferase reporter assay. Lymphatic vessel formation and invasion ability were detected using a lymphatic vessel formation assay and Transwell invasion assay. OIP5-AS1 knockdown attenuated lymphatic vessel length and invasion. The role of OIP5-AS1 was reverted by miR-140-5p. HDAC7 and VEGFA are downstream effectors of miR-140-5p-mediated NSCLC metastasis. OIP5-AS1, miR-140-5p, HDAC7 and VEGFA were all dysregulated in human clinical NSCLC tumor tissues. In conclusion, the present results demonstrated a novel mechanism for OIP5-AS1-induced metastatic phenotypes of NSCLC via the miR-140-5p/HDAC7/VEGFA axis.

Introduction

Lung cancer is one of the most common cancer types with a high mortality rate globally (1). Non-small cell lung cancer (NSCLC) represents a large proportion of lung cancer cases (2). The 5-year survival rate of patients with lung cancer is only 15%, which is due to metastasis (3). Early stage diagnosis of NSCLC might lead to higher survival rates and patients could be effectively treated by surgery, radiotherapy or chemotherapy sooner (4). Therefore, it is important to gain an improved understanding of NSCLC progression.

Long non-coding RNA (lncRNA) is a form of non-coding RNA, ~200 nucleotides in length, that cannot be translated into protein (5). A number of lncRNAs regulate cancer metastasis and progression. In several studies, Opa-interacting protein 5 antisense RNA 1 (OIP5-AS1; transcribed into the antisense strand of OIP5) functions as an oncogenic lncRNA in several cancer types, including oral squamous cell carcinoma (6), bladder cancer (7) and hemangioma (8). OIP5-AS1 was reported to promote lung cancer progression (9,10). Nonetheless, the underlying molecular mechanisms of OIP5-AS1 function in this phenomenon have not been fully elucidated.

MicroRNAs (miRs/miRNAs) are non-coding RNAs ~22 nucleotides in length (11). miRs regulate gene expression levels via occupying 3'-untranslated (3'-UTR) regions of target genes (12). miRs are involved in a number of cancer types, including NSCLC (13,14). miR-140-5p was demonstrated to inhibit proliferation, invasion and drug resistance of NSCLC via the vascular endothelial growth factor A (VEGFA) and Wnt signaling pathways (15,16).

Histone deacetylase 7 (HDAC7) is a class 2 member of the HDAC family (17). Previous studies have shown that HDACs affect gene transcription through complexing with classical transcription factors, such as STAT3, hypoxia-inducible factor-1α, forkhead box protein (FOX) P3 and FOXA1 (18-20). Caslini *et al* (21) suggested that HDAC7 was necessary for stem cell-like properties of breast cancer cells. Additionally, HDAC7 deletion in endothelial progenitor cells repressed the neovascularization of NSCLC tumors via regulating the transcription of angiogenic genes, such as VEGF (22). However, whether HDAC7 exerts a role in NSCLC cells remains to be elucidated.

The present study aimed to investigate and resolve the novel molecular mechanism underlying OIP5-AS1-induced metastasis in NSCLC. These findings may help advance the understanding of NSCLC progression and aid the development of novel therapeutic targets for treating NSCLC.

Materials and methods

Cell lines. Human lung cancer cells (A549 and H1299) were obtained from American Type Culture Collection. Lung cancer cells were cultured in DMEM (HyClone; Cytiva) supplemented

---

Correspondence to: Professor Jiazhuan Mei, Department of Oncology, People's Hospital of Zhengzhou, 33 Huanghe Road, Zhengzhou, Henan 450000, P.R. China
E-mail: jiazhuanmei2020@126.com

with 10% FBS (Hyclone; GE Healthcare Life Sciences) and 1% penicillin/streptomycin at 5% CO_2 and 37°C. In addition, human dermal lymphatic endothelial cells (HDLECs) were obtained from PromoCell GmbH. HDLECs were cultured in endothelial cell growth medium (PromoCell GmbH) at 5% CO_2 and 37°C. After 72 h, the conditioned medium (CM) from A549 and H1299 cells were harvested and filtered. HDLECs ($2x10^5$ per well) were plated in 6-well cell culture plates.

Cell transfection. HDAC7 and VEGFA cDNA sequences were cloned and ligated into a pcDNA6 vector (Youbio Inc., http://www.youbio.cn/). In brief, RNAs were extracted from A549 cells using TRIzol® reagent (Invitrogen; Thermo Fisher Scientific, Inc.). The concentration and purity of RNA were determined using NanoDrop™ 2000 (Thermo Fisher Scientific, Inc.). cDNA was synthesized from 2 µg RNA using the PrimeScript RT kit (Takara Biotechnology Co., Ltd.) at 42°C for 30 min and 85°C for 5 sec. cDNA samples were diluted with 50 µl RNase-free water. HDAC7 and VEGFA cDNA were cloned and amplified by PCR. Q5 High-Fidelity DNA Polymerase (M0491, New England Biolabs Inc.) was used to amplify DNA. HDAC7, forward: 5'-GGTACCATG CACAGCCCCGGCGCTGATGG-3' and reverse: 5'-CTC GAGTTAGAGATTCATAGGTTC-3'; VEGFA, forward: 5'-GGTACCATGACGGACAGACAGACAGACAC-3' and reverse: 5'-CTCGAGTCACCGCCTCGGCTTGTCA-3'. The following thermocycling conditions were used: Initial denaturation at 98°C for 30 sec, followed by 30 cycles of 98°C for 10 sec, 60°C for 20 sec and 72°C for 30 sec with final extension at 72°C for 2 min. The constructed vectors (2 µg), NC mimic (50 µM), NC inhibitor (50 µM), miR-140-5p mimic (50 µM) and miR-140-5p inhibitor (50 µM) were transiently transfected into A549 cells using Lipofectamine® 2000 (Invitrogen; Thermo Fisher Scientific, Inc). NC mimic: 5'-GGUUCCAUC GUACACUGUUCA-3'; miR-140-5p 5'-mimic: CUCACAGAG AAGGGCAGUG-3'; NC inhibitor: 5'-CCAUCAGUCCCC AUCGCCA-3'; miR-140-5p inhibitor: 5'-CAGUAGUAGAAC GGCG-3'. After 48 h of transfection, the cells were used for subsequent experimentation. Transfection efficiency reached 50-70% through visualizing EGFP positive cells under microscopy. Small interfering (si)-negative control (NC) (20 µM), si-OIP5-AS1 (20 µM), miR-140-5p mimic and inhibitor were all synthesized by Shanghai GenePharma Co., Ltd. The sequences were as follows: si-NC: UACCGACUGGCAAUU CAUG; si-OIP5-AS1: GGCAGUAGAAUCACUUAAA and si-HDAC7: GGGCUGACAAAGAAGAAGU.

Gene cloning bacterial transformation. The cDNAs and pcDNA6 vector were double-digested with restriction enzymes (*Kpn*I and *Xho*I) at 37°C for 12 h. The digested linear sequences were ligated using T4 ligase at 16°C for 12 h. The ligated vectors were then transformed into DH5α competent bacteria (Sangon Biotech Co., Ltd). A tube containing ligated vectors and competent bacteria were incubated at 42°C for 90 sec and then placed on ice.

Bioinformatic prediction. Starbase version 2.0 online program (developed by Sun Yat-sen University) was to perform prediction of interaction between OIP5-AS1 and miR-140-5p. TargetScan (developed by the Massachusetts Institute of Technology) was also used to predict interaction between miR-140-5p and HDAC7.

Dual-luciferase reporter assay. Wild-type and mutant sequences of OIP5-AS1 and HDAC7 were subcloned into a pGL3 vector (Promega Corporation). HDAC7 and VEGFA cDNA were cloned and amplified by PCR. Following 12 h of A549 cell inoculation at density of $3x10^4$ cells/well (24-well plate), the vectors were transfected into cells using Lipofectamine® 2000 (Invitrogen; Thermo Fisher Scientific, Inc.). After 48 h, cells were collected. Luciferase activities were determined using a Dual-Luciferase Reporter Assay system (Promega Corporation). Firefly luciferase activity was normalized to *Renilla* luciferase activity.

Transwell invasion assay. H1299 and A549 cells (~$1x10^5$ cells per well) were resuspended in 250 µl DMEM. Cells were plated in the upper chamber containing Matrigel-coated membranes (precoating for 12 h at 4°C). Approximately 300 µl DMEM supplemented with 50% FBS was plated in the bottom chambers. Following incubation for 48 h, invaded cells were stained with 0.005% crystal violet for 2 h at room temperature and visualized under light microscope (magnification, x400).

Reverse transcription-quantitative PCR (RT-qPCR). RNA extraction was performed as aforementioned. Subsequently, 0.5 µl cDNA was used for qPCR in a total volume of 10 µl using the SYBR Green I Master Mix kit (Thermo Fisher Scientific, Inc.) and primers. qPCR was performed on an ABI 7500 instrument (Applied Biosystems; Thermo Fisher Scientific, Inc.). The following thermocycling conditions were used for the two-step qPCR program: Initial denaturation at 94°C for 15 min; followed by 40 cycles of 94°C for 30 sec, 60°C for 30 sec and 70°C for 30 sec. GAPDH served as the internal control for OIP5-AS1, VEGFA and HDAC7, whereas U6 was the internal control for miR-140-5p. Relative gene expression was calculated using $2^{-\Delta\Delta Cq}$ method (23). The following primer pairs were used for the qPCR: OIP5-AS1 forward, 5'-TGCGAAGATGGCGGAGTAAG-3' and reverse, 5'-TAG TTCCTCTCCTCTGGCCG-3'; miR-140-5p forward, 5'-CAG TGGTTTTACCCTATGGTAG-3' and reverse, 5'-ACCATA GGGTAAAACCACTGTT-3'; HDAC7 forward, 5'-TGCTCT TGTCCTTGTGGAGA-3' and reverse, 5'-CCACCACCTCTT CCTAGCAG-3'; VEGFA forward, 5'-GGCCAGCACATA GGAGAGAT-3' and reverse, 5'-ACGCTCCAGGACTTATAC CG-3'; GAPDH forward, 5'-CTGACTTCAACAGCGACA CC-3' and reverse, 5'TGCTGTAGCCAAATTCGTTG-3'; U6 forward, 5'CGCTTCGGCAGCACATATACTA-3' and reverse, 5'GAATTTGCGTGTCATCCTTGCG-3'.

Lymphatic vessel formation assay. HDLECs were subjected to CM treatment on Growth Factor Reduced Matrigel. Matrigel was diluted with PBS buffer at a 1:5 ratio. The resultant solution was used to coat 24-well plates (0.2 ml/well) and incubated at 37°C for 5 h. HDLECs were cultured in DMEM in wells at a density of ~$5x10^4$ cells/well. When experiment was finished (6 h after incubation), an inverted microscope (magnification, x400) was used to observe and capture images. Mean tube lengths were quantified (normalized to the control) using the Image-Pro® Plus software (Media Cybernetics, Inc.).

Western blotting. Total protein was extracted from A549 cells using 1x RIPA buffer (Beyotime Institute of Biotechnology). The protein concentration of supernatant was determined using the bicinchoninic acid method. Approximately 50 μg protein/lane were separated by 10% SDS-PAGE. The separated proteins were then transferred to a nitrocellulose membrane (EMD Millipore). Blocking was performed using 5% non-fat milk for 1 h at room temperature. Subsequently, the immunoblotted membrane was incubated with the following primary antibodies: Anti-HDAC7 (cat. no. ab50212, 1:1,000, Abcam), anti-VEGFA (cat. no. ab51745, 1:1,000, Abcam) and anti-GAPDH (cat. no. GTX124502, 1:1,000, GeneTex Inc.) overnight at 4˚C. The following day, the membrane was washed with PBS-Tween-20 (0.05%) (PBS-T) and incubated with secondary antibodies for 1 h at room temperature. anti-mouse IgG-HRP (cat. no. SE131, 1:2,000, Beijing Solarbio Science & Technology Co., Ltd.), anti-rabbit IgG-HRP (cat. no. SE134, 1:2,000. Beijing Solarbio Science & Technology Co., Ltd.). After washing with PBS-T, protein signal intensity was measured using an ECL exposure system.

The Cancer Genome Atlas (TCGA) analysis. The gene expression datasets of lung tumors were downloaded from the Genomic Data Commons (GDC) lung adenocarcinoma TCGA datasets (160 cancer and 369 normal tissues). The datasets used were originally from api.gdc.cancer.gov/data/. For stage plot analysis, we grouped the patients according to stage I, II, III and IV lung cancer. Then, we input genes (OIP5-AS1, miR-140-5p, HDAC7, VEGFA) expression data into GraphPad Prism (GraphPad Software) to draw the stage plot. For Kaplan-Meier plot analysis, the clinical information of survival was used to draw survival curve using GraphPad Prism software.

Statistical analysis. GraphPad Prism 8.0 (GraphPad Software, Inc.) was used to perform statistical analysis. The data of three replicates were calculated as the mean ± SD. Comparisons between two or more experimental groups were analyzed using unpaired Student's t-test and one-way ANOVA with Tukey's post hoc test. Lung tumor tissues and paired adjacent normal tissues of TCGA were evaluated using paired Student's t-test. $P < 0.05$ was considered to indicate a statistically significant difference.

Results

OIP5-AS1 promotes NSCLC metastasis. To determine the role of OIP5-AS1 in NSCLC metastasis, TCGA datasets of NSCLC were analyzed. OIP5-AS1 was significantly upregulated in lung tumor tissues compared with normal tissues (Fig. 1A). Moreover, higher levels of OIP5-AS1 were observed in advanced stages of NSCLC tumors (stage III and IV) compared with lower stages of tumors (stage I and II) (Fig. 1B). Low levels of OIP5-AS1 were associated with higher overall survival rate of patients with NSCLC (Fig. 1C).

Next, OIP5-AS1 knockdown in H1299 and A549 cells was performed, and RT-qPCR analysis showed that OIP5-AS1 levels significantly decreased in si-OIP-AS1 groups compared with si-NC groups (Fig. 1D). Compared with si-NC groups, OIP5-AS1 knockdown led to a significant reduction in lymphatic vessel formation ability in HDLECs incubated with H1299 or A549 CM (Fig. 1E and F). Likewise, OIP5-AS1 knockdown attenuated the invasion of H1299 or A549 cells compared with the si-NC group (Fig. 1G). These data showed that OIP5-AS1 plays a role in NSCLC progression.

miR-140-5p rescues OIP5-AS1-induced NSCLC metastasis. miRNAs were reported to function in several cancer types by being sponged by lncRNAs (24-26). Based on these findings, the present study aimed to identify potential miRNAs responsible for OIP5-AS1-enhanced NSCLC progression. miR-140-5p was identified as the candidate gene using bioinformatics analysis (Fig. 2A). To validate the findings, a dual-luciferase reporter assay was performed using A549 cells, as this is the most used cell line in previous stduies investigating lung cancer (27,28). The results demonstrated that the miR-140-5p mimic significantly reduced the luciferase activity of A549 cells compared with NC mimic, whereas miR-140-5p inhibitor significantly increased luciferase activity compared with the NC inhibitor group. There is no significant alteration in mutant OIP5-AS1-expressing A549 cells (Fig. 2B). Furthermore, miR-140-5p mimic significantly reduced OIP5-AS1 expression levels compared with the NC mimic group, while miR-140-5p inhibitor significantly increased OIP5-AS1 expression levels compared with the NC inhibitor group. The miR-140-5p mimic greatly increased miR-140-5p levels and the miR-140-5p inhibitor downregulated miR-140-5p expression (Fig. 2C). Clinically, it was found that miR-140-5p levels were significantly lower in NSCLC tumors compared with normal tissues (Fig. 2D).

To investigate the role of miR-140-5p in OIP5-AS1-regulated metastasis, miR-140-5p levels were examined in A549 cells treated with si-OIP5-AS1, si-OIP5-AS1 plus miR-140-5p inhibitor. si-OIP5-AS1 increased miR-140-5p levels by 4-fold and miR-140-5p inhibitor restored miR-140-5p levels compared with the si-NC (Fig. 2E). Transfection with si-OIP5-AS1 attenuated the lymphatic vessel formation ability in HDLECs cultured with A549 medium, which was partly rescued by miR-140-5p inhibitor (Fig. 2F and G). OIP5-AS1 knockdown reduced cell invasion compared with the si-NC group. Cell invasion was rescued by miR-140-5p inhibitor (Fig. 2H). Taken together, these data demonstrated that miR-140-5p is a mediator of OIP5-AS1-regulated NSCLC metastasis.

HDAC7 is involved in miR-140-5p-modulated metastatic phenotypes of NSCLC. The aforementioned findings led to the investigation of the downstream targets of miR-140-5p in NSCLC. TargetScan was used and predicted the epigenetic regulator HDAC7 as a potential candidate (Fig. 3A). The dual-luciferase reporter assay results showed that compared with their respective NC groups, miR-140-5p mimic significantly reduced luciferase activity of A549 cells containing the wild-type 3'-UTR of HDAC7, whereas miR-140-5p inhibitor significantly increased luciferase activity. There is no significant alteration in mutant 3'-UTR of HDAC7-expressing A549 cells (Fig. 3B). Compared with their respective NC groups, western blotting results demonstrated miR-140-5p mimic attenuated HDAC7 protein levels, while miR-140-5p inhibitor increased HDAC7 protein levels (Fig. 3C). In addition, HDAC7 levels were significantly higher in NSCLC tumors compared with normal adjacent tissues (Fig. 3D).
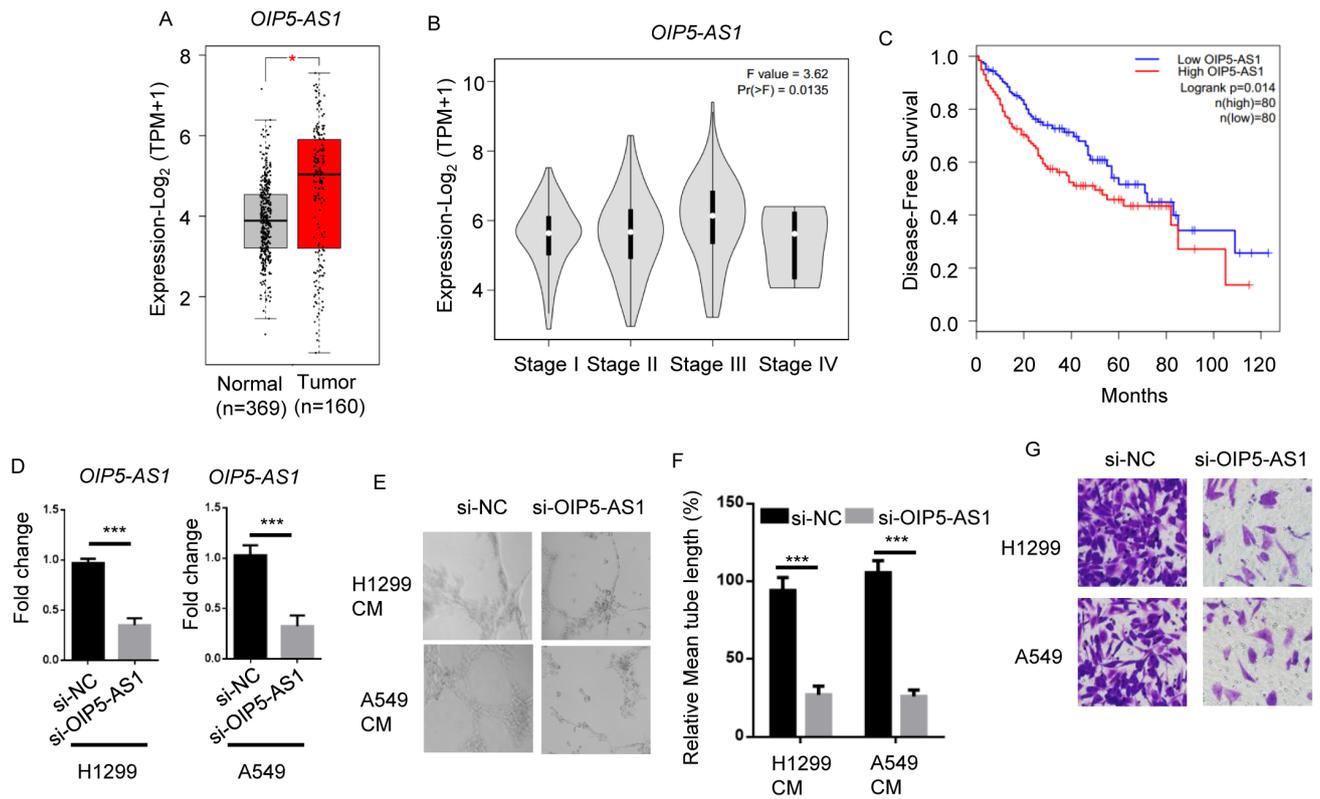
Figure 1. OIP5-AS1 promotes NSCLC metastasis. (A) Bioinformatic analysis of The Cancer Genome Atlas datasets showed OIP5-AS1 levels in human normal lung tissues (n=369) or lung adenocarcinoma tumors (n=160). (B) Stage plot showing that OIP5-AS1 levels were associated with advanced stages of patients with NSCLC. F=3.62, P=0.0135. (C) Kaplan-Meier plot showed the overall survival rate of patients with lung adenocarcinoma. P=0.014, n (high) =80, n (low) =80. (D) Reverse transcription-quantitative PCR showing OIP5-AS1 levels in H1299 or A549 cells transfected with si-NC or si-OIP5-AS. (E) Representative microscopy images (400x magnification) and (F) quantification (normalized to the control) of lymphatic vessel formation in human dermal lymphatic endothelial cells cultured with conditioned medium of H1299 or A549 cells transfected with si-NC or si-OIP5-AS1. (G) Transwell assay showing invasion of H1299 or A549 cells transfected with si-NC or si-OIP5-AS1 (400x magnification). Data are presented as the mean ± standard deviation. *P<0.05; ***P<0.001. OIP5-AS1, Opa-interacting protein 5 antisense RNA 1; NSCLC, non-small cell lung cancer; si, small interfering; NC, negative control; TPM, Transcripts Per Million.

To evaluate whether HDAC7 plays a role in miR-140-5p-regulated metastasis, HDAC7 was elevated by ~24-fold in pcDNA6-HDAC7-transfected A549 cells compared with pcDNA6-transfected A549 cells. Meanwhile, miR-140-5p mimic downregulated HDAC7 expression and HDAC7 overexpression in miR-140-5p mimic-transfected A549 cells resulted in 4-5-fold upregulation of HDAC7 compared with the NC mimic (Fig. 3E and F). Compared with the NC mimic group, miR-140-5p mimic significantly decreased the lymphatic vessel formation ability of HDLECs incubated with A549 medium, which was rescued by HDAC7 overexpression (Fig. 3G and H). miR-140-5p mimic reduced the number of invaded cells, and this trend was enhanced by HDAC7 (Fig. 3I). The results suggested that HDAC7 plays a role miR-140-5p-inhibited NSCLC metastasis.

VEGFA acts as an effector for HDAC7-regulated NSCLC metastasis. It was recently reported that HDAC7 contributed to cancer progression via regulating VEGFA expression levels (21). VEGFA has also been shown to be implicated in cancer metastasis (29,30). Thus, it was hypothesized that VEGFA acted as a downstream effector for the OIP5-AS1/miR-140-5p/HDAC7 axis in NSCLC cells. RT-qPCR and western blotting were performed to analyze VEGFA expression levels in HDAC7-knockdown A549 cells (Fig. 4A and B). HDAC7 expression was markedly

reduced in A549 cells transfected with si-HDAC7 compared with si-NC. Consistent with previous results, HDAC7 knockdown resulted in downregulation of VEGFA levels compared with the si-NC group. VEGFA expression levels were significantly upregulated in NSCLC tumors compared with normal adjacent tissues (Fig. 4C).

To assess the function of VEGFA in NSCLC, VEGFA was overexpressed in HDAC7-depleted A549 cells (Fig. 4D and E). HDAC7 knockdown impaired lymphatic vessel formation of HDLEC cells incubated with A549 medium; however, VEGFA overexpression significantly restored this phenotype (Fig. 4F and G). In addition, si-HDAC7 cells reduced invasion ability compared with the si-NC group, which was reverted by VEGFA overexpression (Fig. 4H). The results suggested that VEGFA plays a role in OIP5-AS1/miR-140-5p/HDAC7 axis-induced tumor metastasis of NSCLC.

Discussion

The present study demonstrated that OIP5-AS1 negatively interacted with miR-140-5p, thereby regulating HDAC7 and VEGFA expression levels (Fig. 5). miR-140-5p functioned as an effector for the biological role of OIP5-AS1 in lung cancer cell metastasis. HDAC7 and VEGFA rescued OIP5-AS1/miR-140-5p-related tumor phenotypes, and it was
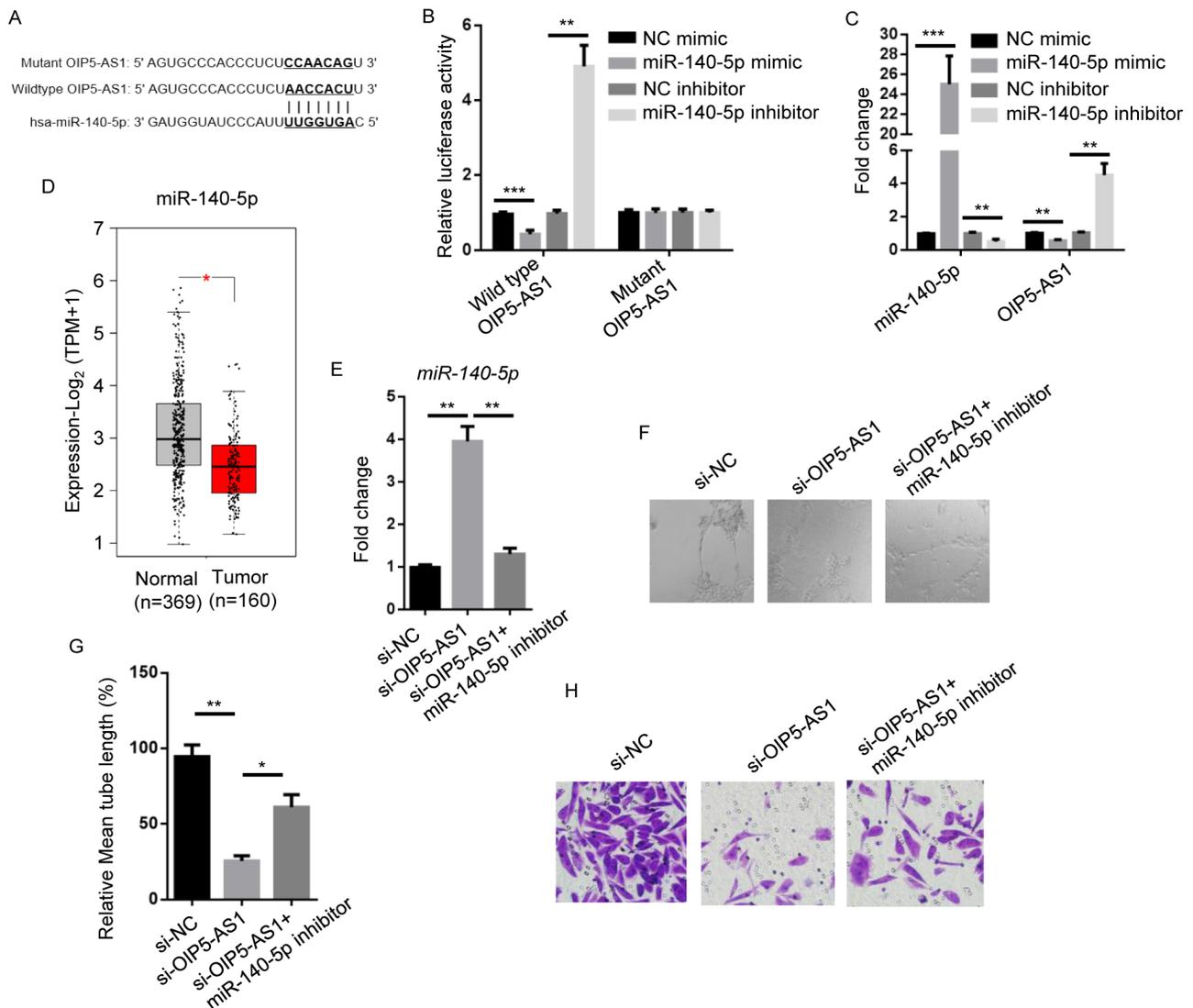
Figure 2. miR-140-5p rescues OIP5-AS1-regulated NSCLC metastasis. (A) Bioinformatics analysis showing the binding site of OIP5-AS1 by miR-140-5p. Complementary sequences are shown in bold. (B) Luciferase activity in A549 cells transfected with NC mimic, miR-140-5p mimic, NC inhibitor and miR-140-5p inhibitor. (C) RT-qPCR showing miR-140-5p and OIP5-AS1 expression levels in A549 cells transfected with NC mimic, miR-140-5p mimic, NC inhibitor and miR-140-5p inhibitor. (D) Bioinformatic analysis of The Cancer Genome Atlas datasets showing miR-140-5p levels in human normal lung tissues (n=369) or lung adenocarcinoma tumors (n=160). (E) RT-qPCR showing miR-140-5p levels in A549 cells transfected with si-NC, si-OIP5-AS1 or si-OIP5-AS1 + miR-140-5p inhibitor. (F) Representative microscopy images (400x magnification) and (G) quantification (normalized to the control) of lymphatic vessel formation in human dermal lymphatic endothelial cells cultured with conditioned medium of A549 cells transfected with si-NC, si-OIP5-AS1 or si-OIP5-AS1 + miR-140-5p inhibitor. (H) Transwell assay showing invasion of A549 cells transfected with si-NC, si-OIP5-AS1 or si-OIP5-AS1 + miR-140-5p inhibitor (400x magnification). Data are presented as the mean ± standard deviation. $^{*}P<0.05$; $^{**}P<0.01$ and $^{***}P<0.001$. miR, microRNA; OIP5-AS1, Opa-interacting protein 5 antisense RNA 1; NSCLC, non-small cell lung cancer; NC, negative control; RT-qPCR, reverse transcription-quantitative PCR; si, small interfering; TPM, Transcripts Per Million.

observed that the OIP5-AS1/miR-140-5p/HDAC7 axis was dysregulated in TCGA lung tumors.

Generally, patients with NSCLC are treated with chemotherapy agents, such as cisplatin, for most cases (31). Although the overall survival rate of patients with NSCLC has improved recently, the therapeutic effect of chemotherapy reaches a plateau with a 20% response rate and median survival of 8-10 months (32). More notably, molecular targeted therapy is one of the most novel strategies for NSCLC treatment, such as epidermal growth factor receptor (EGFR) mutation and anaplastic lymphoma kinase (ALK) rearrangement (33). Gefitinib and crizotinib are the two targeted drugs for EGFR and ALK tyrosine kinase inhibitors, respectively (33). In the

present study, it was confirmed that OIP5-AS1 exerted a role in NSCLC progression, suggesting that OIP5-AS1 may have value as a diagnostic biomarker and therapeutic target for NSCLC treatment.

LncRNAs function as endogenous miRNA decoys in cancer to modulate the expression of downstream target genes (34). It was shown that OIP5-AS1 acts as a competitive endogenous RNA for sponging miRNAs, such as miR-338-3p (6), miR-448 (9) and miR-378a-3p (10). In the present study, we demonstrated that OIP5-AS1 negatively regulated miR-140-5p by complementary binding.

A study indicated that miR-140-5p suppressed the migration, proliferation and invasion of NSCLC cells (14). The lncRNA HANR
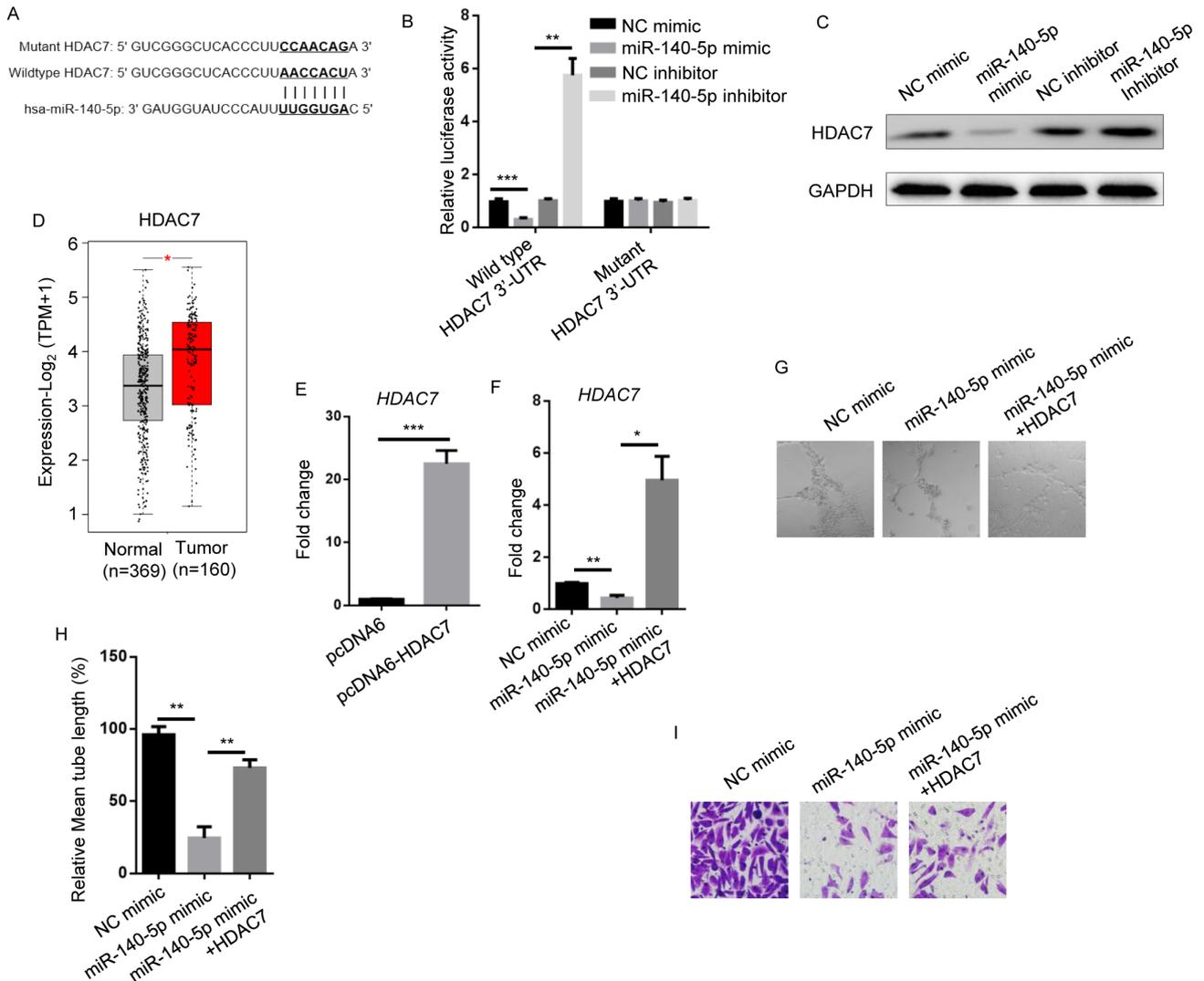
Figure 3. HDAC7 is involved in miR-140-5p-modulated metastatic phenotypes of non-small cell lung cancer. (A) Bioinformatics of the putative binding site at the 3'-UTR of HDAC7 by miR-140-5p. Complementary sequences are shown in bold. (B) Luciferase activity in A549 cells transfected with NC mimic, miR-140-5p mimic, NC inhibitor and miR-140-5p inhibitor. (C) Western blotting showing HDAC7 expression levels in A549 cells transfected with NC mimic, miR-140-5p mimic, NC inhibitor and miR-140-5p inhibitor. GAPDH was the internal control. (D) Bioinformatic analysis of The Cancer Genome Atlas datasets showing HDAC7 levels in human normal lung tissues (n=369) or lung adenocarcinoma tumors (n=160). Reverse transcription-quantitative PCR showing HDAC7 levels in A549 cells transfected with (E) pcDNA6 and pcDNA6-HDAC7 and (F) NC mimic, miR-140-5p mimic and miR-140-5p mimic + HDAC7. (G) Representative microscopy images (400x magnification) and (H) quantification (normalized to the control) of lymphatic vessel formation in human dermal lymphatic endothelial cells cultured with conditioned medium of A549 cells transfected with NC mimic, miR-140-5p mimic and miR-140-5p mimic + HDAC7. (I) Transwell invasion assay showing invasion of A549 cells transfected with NC mimic, miR-140-5p mimic and miR-140-5p mimic + HDAC7 (400x magnification). Data are presented as the mean ± standard deviation. $^*P<0.05$; $^{**}P<0.01$ and $^{***}P<0.001$. HDAC7, human dermal lymphatic endothelial cells; miR, microRNA; NC, negative control; 3'UTR, 3'-untranslated region; TPM, Transcripts Per Million.

negatively regulated miR-140-5p to aggravate the proliferation, migration and invasion of NSCLC (35). Consistently, the present study found that miR-140-5p inhibited the invasion and lymphatic vessel formation ability of A549 cells. In addition, miR-140-5p levels were relatively lower in human clinical lung tumors tissues compared with normal tissues. Additionally, miR-140-5p was shown to partly restore OIP5-AS1-induced phenotypes.

HDAC7 is a member of the HDAC family. Commonly, HDAC7 upregulates the acetylation of histones (especially H3) in an enzymatic activity-dependent manner, thereby activating the expression of target genes (36). However, HDAC7 also exerts non-enzymatic dependent activity, instead functioning via interaction with other transcriptional factors (18,37). The present data showed that HDAC7 positively regulated VEGFA, which is in

agreement with previously published study (21). Caslini *et al* (21), indicated that HDAC7 reduced *H3K27ac*, a super enhancer-related gene, levels in human breast cancer cells. Caslini *et al* reported that HDAC7-knockdown influenced chromatin configuration and blocked the expression of oncogenes. Moreover, the present results confirmed the regulatory relationship between HDAC7 and VEGFA using RT-qPCR and western blot analysis.

VEGF was shown to induce angiogenesis in a VEGFR2-dependent manner, which is important for tumor metastasis (38). Recently, homeoprotein Six1, a member of Six family of homeodomain transcription factors, enhanced colorectal cancer metastasis and angiogenesis via upregulating VEGF (39). miR-195 inhibited VEGF to regulate squamous cell lung cancer metastasis and angiogenesis (40). Sinha *et al* (41)
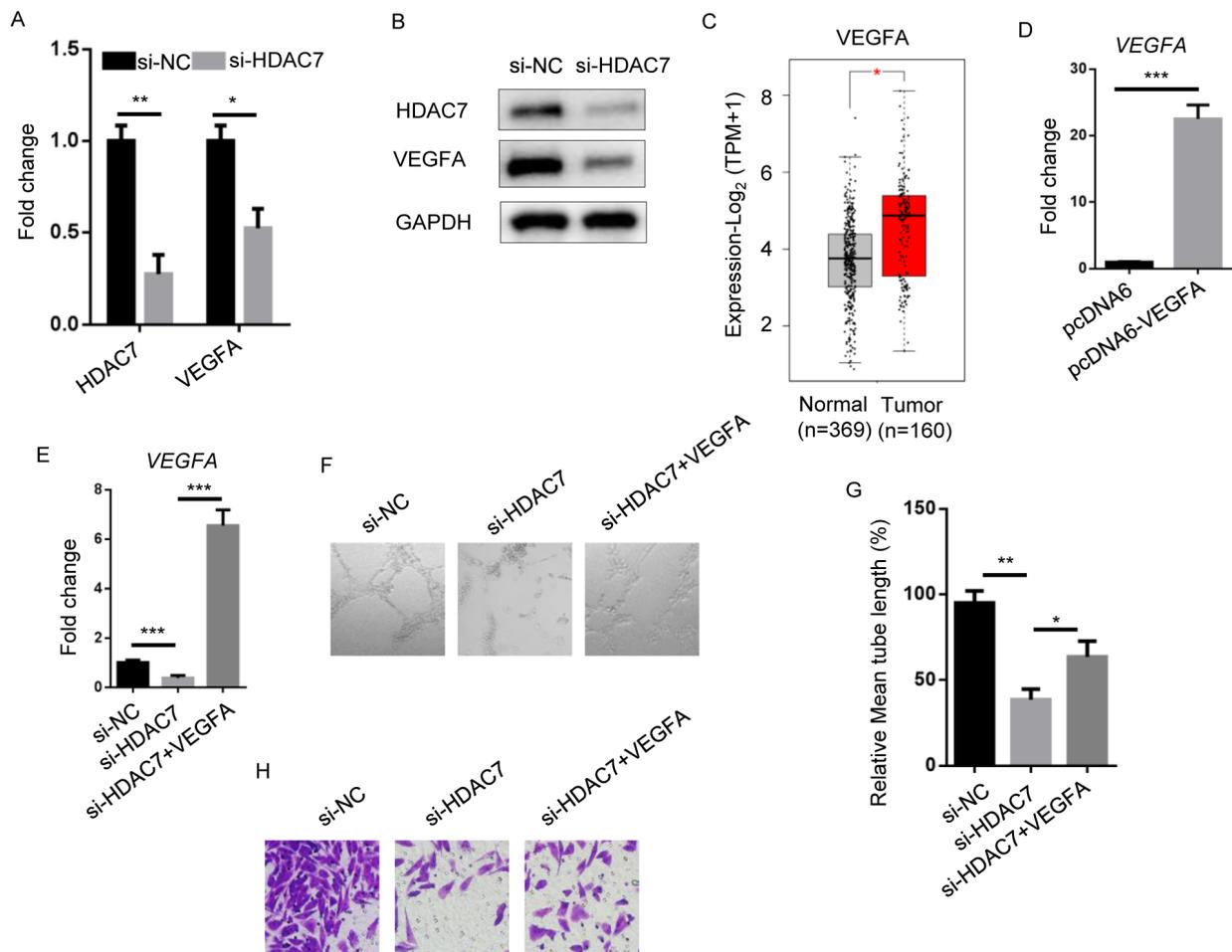
Figure 4. VEGFA functions as an effector for HDAC7-regulated non-small cell lung cancer metastasis. (A) RT-qPCR showing HDAC7 and VEGFA levels in A549 cells transfected with si-NC and si-HDAC7. (B) Western blotting of HDAC7 and VEGFA levels in A549 cells transfected with si-NC and si-HDAC7. GAPDH was the internal control. (C) Bioinformatic analysis of The Cancer Genome Atlas datasets showing VEGFA levels in human normal lung tissues (n=369) or lung adenocarcinoma tumors (n=160). RT-qPCR showing VEGFA levels in A549 cells transfected with (D) pcDNA6 and pcDNA-VEGFA and (E) si-NC, si-HDAC7 and si-HDAC7 + VEGFA. (F) Representative microscopy images (400x magnification) and (G) quantification (normalized to the control) of lymphatic vessel formation in human dermal lymphatic endothelial cells cultured with conditioned medium of A549 cells transfected with si-NC, si-HDAC7 and si-HDAC7 + VEGFA. (H) Transwell invasion assay showing invasion of A549 cells transfected with si-NC, si-HDAC7 and si-HDAC7 + VEGFA (400x magnification). Data are presented as the mean ± standard deviation. *P<0.05; **P<0.01 and ***P<0.001. HDAC7, human dermal lymphatic endothelial cells; RT-qPCR, reverse transcription-quantitative PCR; si, small interfering; NC, negative control; HDAC7, human dermal lymphatic endothelial cells; VEGFA, vascular endothelial growth factor A; TPM, Transcripts Per Million.
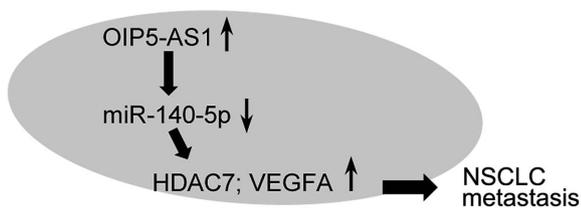
Figure 5. Model of OIP5-AS1-modulated NSCLC metastasis. OIP5-AS1 promoted HDAC7 and VEGFA expression via binding miR-140-5p, subsequently contributing to NSCLC metastasis. OIP5-AS1, Opa-interacting protein 5 antisense RNA 1; NSCLC, non-small cell lung cancer; HDAC7, human dermal lymphatic endothelial cells; VEGFA, vascular endothelial growth factor A; miR-140-5p, microRNA-140-5p.

suggested that VEGF was involved in breast cancer metastasis and angiogenesis via the focal adhesion kinase/matrix metalloproteinase-9 signaling pathway. In agreement with the present data, it was also observed that VEGFA promoted lung cancer invasion and lymphatic vessel formation.

In summary, the present study suggested the oncogenic role of lncRNA OIP5-AS1 in NSCLC metastasis via miR-140-5p at the cellular and clinical levels. HDAC7 and VEGFA are two downstream effectors for mediating OIP5-AS1/miR-140-5p-regulated NSCLC metastasis. The present findings may provide an improved understanding of NSCLC progression and accelerate the development of diagnostic and therapeutic strategies for the treatment of NSCLC.

Acknowledgements

Funding

Availability of data and materials

The datasets analyzed in this study are available in The Cancer Genome Atlas, (https://cancergenome.nih.gov/).

Authors' contributions

JM conceived and designed the experiments, and wrote the manuscript. GL, WW, PX and DY performed the experiments. HB and RL analyzed the data. All authors read and approved the final manuscript.

Ethics approval and consent to participate

Not applicable.

Patient consent for publication

Not applicable.

Competing interests

The authors declare that they have no competing interests.

References

1. Zhuang Y, Jiang H, Li H, Dai J, Liu Y, Li Y, Miao L, Cai H, Xiao Y, Xia H, *et al*: Down-regulation of long non-coding RNA AFAP1-AS1 inhibits tumor cell growth and invasion in lung adenocarcinoma. Am J Transl Res 9: 2997-3005, 2017.
2. Herbst RS, Morgensztern D and Boshoff C: The biology and management of non-small cell lung cancer. Nature 553: 446-454, 2018.
3. Zhou C, Wu YL, Chen G, Feng J, Liu XQ, Wang C, Zhang S, Wang J, Zhou S, Ren S, *et al*: Erlotinib versus chemotherapy as first-line treatment for patients with advanced EGFR mutation-positive non-small-cell lung cancer (OPTIMAL, CTONG-0802): A multicentre, open-label, randomised, phase 3 study. Lancet Oncol 12: 735-742, 2011.
4. Morgensztern D, Ng SH, Gao F and Govindan R: Trends in stage distribution for patients with non-small cell lung cancer: A national cancer database survey. J Thorac Oncol 5: 29-33, 2010.
5. Xu G, Chen J, Pan Q, Huang K, Pan J, Zhang W, Chen J, Yu F, Zhou T and Wang Y: Long noncoding RNA expression profiles of lung adenocarcinoma ascertained by microarray analysis. PLoS One 9: e104044, 2014.
6. Li M, Ning J, Li Z, Fei Q, Zhao C, Ge Y and Wang L: Long noncoding RNA OIP5-AS1 promotes the progression of oral squamous cell carcinoma via regulating miR-338-3p/NRP1 axis. Biomed Pharmacother 118: 109259, 2019.
7. Wang Y, Shi F, Xia Y and Zhao H: LncRNA OIP5-AS1 predicts poor prognosis and regulates cell proliferation and apoptosis in bladder cancer. J Cell Biochem 2018 (Online ahead of print).
8. Zhang J, Zhao T, Tian L and Li Y: LncRNA OIP5-AS1 promotes the proliferation of hemangioma vascular endothelial cells via regulating miR-195-5p/NOB1 axis. Front Pharmacol 10: 449, 2019.
9. Deng J, Deng H, Liu C, Liang Y and Wang S: Long non-coding RNA OIP5-AS1 functions as an oncogene in lung adenocarcinoma through targeting miR-448/Bcl-2. Biomed Pharmacother 98: 102-110, 2018.
10. Wang M, Sun X, Yang Y and Jiao W: Long non-coding RNA OIP5-AS1 promotes proliferation of lung cancer cells and leads to poor prognosis by targeting miR-378a-3p. Thorac Cancer 9: 939-949, 2018.
11. Acunzo M, Romano G, Wernicke D and Croce CM: MicroRNA and cancer-a brief overview. Adv Biol Regul 57: 1-9, 2015.
12. Yao Y, Ma J, Xue Y, Wang P, Li Z, Liu J, Chen L, Xi Z, Teng H, Wang Z, *et al*: Knockdown of long non-coding RNA XIST exerts tumor-suppressive functions in human glioblastoma stem cells by up-regulating miR-152. Cancer Lett 359: 75-86, 2015.
13. Sun Y and Qin B: Long noncoding RNA MALAT1 regulates HDAC4-mediated proliferation and apoptosis via decoying of miR-140-5p in osteosarcoma cells. Cancer Med 7: 4584-4597, 2018.
14. Zhou W, Wang X, Yin D, Xue L, Ma Z, Wang Z, Zhang Q, Zhao Z, Wang H, Sun Y and Yang Y: Effect of miR-140-5p on the regulation of proliferation and apoptosis in NSCLC and its underlying mechanism. Exp Ther Med 18: 1350-1356, 2019.
15. Shi SL and Zhang ZH: Long non-coding RNA SNHG1 contributes to cisplatin resistance in non-small cell lung cancer by regulating miR-140-5p/Wnt/β-catenin pathway. Neoplasma 66: 756-765, 2019.
16. Yang P, Xiong J, Zuo L, Liu K and Zhang H: miR1405p regulates cell migration and invasion of nonsmall cell lung cancer cells through targeting VEGFA. Mol Med Rep 18: 2866-2872, 2018.
17. Witt O, Deubzer HE, Milde T and Oehme I: HDAC family: What are the cancer relevant targets? Cancer Lett 277: 8-21, 2009.
18. Jensen ED, Schroeder TM, Bailey J, Gopalakrishnan R and Westendorf JJ: Histone deacetylase 7 associates with Runx2 and represses its activity during osteoblast maturation in a deacetylation-independent manner. J Bone Miner Res 23: 361-372, 2008.
19. Kato H, Tamamizu-Kato S and Shibasaki F: Histone deacetylase 7 associates with hypoxia-inducible factor 1alpha and increases transcriptional activity. J Biol Chem 279: 41966-41974, 2004.
20. Li B, Samanta A, Song X, Iacono KT, Bembas K, Tao R, Basu S, Riley JL, Hancock WW, Shen Y, *et al*: FOXP3 interactions with histone acetyltransferase and class II histone deacetylases are required for repression. Proc Natl Acad Sci USA 104: 4571-4576, 2007.
21. Caslini C, Hong S, Ban YJ, Chen XS and Ince TA: HDAC7 regulates histone 3 lysine 27 acetylation and transcriptional activity at super-enhancer-associated genes in breast cancer stem cells. Oncogene 38: 6599-6614, 2019.
22. Wei Y, Zhou F, Zhou H, Huang J, Yu D and Wu G: Endothelial progenitor cells contribute to neovascularization of non-small cell lung cancer via histone deacetylase 7-mediated cytoskeleton regulation and angiogenic genes transcription. Int J Cancer 143: 657-667, 2018.
23. Livak KJ and Schmittgen TD: Analysis of relative gene expression data using real-time quantitative PCR and the 2(-Delta Delta C(T)) method. Methods 25: 402-408, 2001.
24. Lei H, Gao Y and Xu X: LncRNA TUG1 influences papillary thyroid cancer cell proliferation, migration and EMT formation through targeting miR-145. Acta Biochim Biophys Sin (Shanghai) 49: 588-597, 2017.
25. Yu Y, Shen HM, Fang DM, Meng QJ and Xin YH. LncRNA HCP5 promotes the development of cervical cancer by regulating MACC1 via suppression of microRNA-15a. Eur Rev Med Pharmacol Sci 22: 4812-4819, 2018.
26. Yao N, Yu L, Zhu B, Gan HY and Guo BQ: LncRNA GIHCG promotes development of ovarian cancer by regulating microRNA-429. Eur Rev Med Pharmacol Sci 22: 8127-8134, 2018.
27. Gobillot TA, Humes D, Sharma A, Kikawa C and Overbaugh J: The robust restriction of zika virus by type-I interferon in A549 cells varies by viral lineage and is not determined by IFITM3. Viruses 12: 503, 2020.
28. Massa D, Baran M, Bengoechea JA and Bowie AG: PYHIN1 regulates pro-inflammatory cytokine induction rather than innate immune DNA sensing in airway epithelial cells. J Biol Chem 295: 4438-4450, 2020.
29. Zhang Q, Lu S, Li T, Yu L, Zhang Y, Zeng H, Qian X, Bi J and Lin Y: ACE2 inhibits breast cancer angiogenesis via suppressing the VEGFa/VEGFR2/ERK pathway. J Exp Clin Cancer Res 38: 173, 2019.
30. Guo J, Chen M, Ai G, Mao W, Li H and Zhou J: Hsa_circ_0023404 enhances cervical cancer metastasis and chemoresistance through VEGFA and autophagy signaling by sponging miR-5047. Biomed Pharmacother 115: 108957, 2019.
31. Duma N, Santana-Davila R and Molina JR: Non-small cell lung cancer: Epidemiology, screening, diagnosis, and treatment. Mayo Clin Proc 94: 1623-1640, 2019.
32. Schiller JH, Harrington D, Belani CP, Langer C, Sandler A, Krook J, Zhu J and Johnson DH; Eastern Cooperative Oncology: Comparison of four chemotherapy regimens for advanced non-small-cell lung cancer. N Engl J Med 346: 92-98, 2002.
33. Kumarakulasinghe NB, van Zanwijk N and Soo RA: Molecular targeted therapy in the treatment of advanced stage non-small cell lung cancer (NSCLC). Respirology 20: 370-378, 2015.

34. Cao MX, Jiang YP, Tang YL and Liang XH: The crosstalk between lncRNA and microRNA in cancer metastasis: Orchestrating the epithelial-mesenchymal plasticity. Oncotarget 8: 12472-12483, 2017.

35. Li SJ, Wu YX, Liang YH, Gao Y, Wu AB, Zheng HY and Yang ZX: LncRNA HANR aggravates the progression of non-small cell lung cancer via mediating miRNA-140-5p. Eur Rev Med Pharmacol Sci 24: 704-711, 2020.

36. Dressel U, Bailey PJ, Wang SC, Downes M, Evans RM and Muscat GE: A dynamic role for HDAC7 in MEF2-mediated muscle differentiation. J Biol Chem 276: 17007-17013, 2001.

37. Ma C and D'Mello SR: Neuroprotection by histone deacetylase-7 (HDAC7) occurs by inhibition of c-jun expression through a deacetylase-independent mechanism. J Biol Chem 286: 4819-4828, 2011.

38. Saharinen P, Eklund L, Pulkki K, Bono P and Alitalo K: VEGF and angiopoietin signaling in tumor angiogenesis and metastasis. Trends Mol Med 17: 347-362, 2011.

39. Xu H, Zhang Y, Pena MM, Pirisi L and Creek KE: Six1 promotes colorectal cancer growth and metastasis by stimulating angiogenesis and recruiting tumor-associated macrophages. Carcinogenesis 38: 281-292, 2017.

40. Liu H, Chen Y, Li Y, Li C, Qin T, Bai M, Zhang Z, Jia R, Su Y and Wang C: miR195 suppresses metastasis and angiogenesis of squamous cell lung cancer by inhibiting the expression of VEGF. Mol Med Rep 20: 2625-2632, 2019.

41. Sinha S, Khan S, Shukla S, Lakra AD, Kumar S, Das G, Maurya R and Meeran SM: Cucurbitacin B inhibits breast cancer metastasis and angiogenesis through VEGF-mediated suppression of FAK/MMP-9 signaling axis. Int J Biochem Cell Biol 77: 41-56, 2016.